Automatic Detection and Classification of Convulsive Psychogenic Nonepileptic Seizures Using a Wearable Device

Jayavardhana Gubbi, *Senior Member, IEEE*, Shitanshu Kusmakar, *Student Member, IEEE*, Aravinda S. Rao, *Student Member, IEEE*, Bernard Yan, Terence O'Brien, and Marimuthu Palaniswami, *Fellow, IEEE*

***Abstract*—Epilepsy is one of the most common neurological disorders and patients suffer from unprovoked seizures. In contrast, psychogenic nonepileptic seizures (PNES) are another class of seizures that are involuntary events not caused by abnormal electrical discharges but are a manifestation of psychological distress. The similarity of these two types of seizures poses diagnostic challenges that often leads in delayed diagnosis of PNES. Further, the diagnosis of PNES involves high-cost hospital admission and monitoring using video-electroencephalogram machines. A wearable device that can monitor the patient in natural setting is a desired solution for diagnosis of convulsive PNES. A wearable device with an accelerometer sensor is proposed as a new solution in the detection and diagnosis of PNES. The seizure detection algorithm and PNES classification algorithm are developed. The developed algorithms are tested on data collected from convulsive epileptic patients. A very high seizure detection rate is achieved with 100% sensitivity and few false alarms. A leave-one-out error of 6.67% is achieved in PNES classification, demonstrating the usefulness of wearable device in the diagnosis of PNES.**

***Index Terms*—Accelerometry, epileptic seizure (ES), psychogenic nonepileptic seizure (PNES), support vector machines (SVMs), wavelets.**

I. Introduction

SEVERAL neurological disorders affect the motor system in the brain, resulting in deprivation of purposeful movement and affecting normal interaction with the environment. Epilepsy is one of the most common neurological disorders, affecting about 50 million people worldwide [1]. Patients with epilepsy suffer recurrent unprovoked seizures, which are a transient neurological event caused by excessive or hypersynchronous neuronal network activity in the brain. Seizures carry a significant risk of mortality and morbidity and may on occasions be prolonged and require emergency intervention. One of the greatest disabilities associated with epilepsy is the unpredictability of seizures—which can occur anywhere and anytime. Seizures have been characterized by a variety of symptoms [2]. Another class of seizures known as psychogenic nonepileptic seizures (PNES) are involuntary events that pose diagnostic challenges due to the similarities with epileptic seizures (ES). PNES, commonly called pseudoseizures, are a relatively uncommon disorder with a prevalence of around 1 to 33 cases per $100\,000$ and they account for 5–20% of patients thought to have epilepsy [3]. There is potential for severe harm from the adverse side effects or teratogenicity of antiepileptic drugs prescribed to PNES patients [4], as well as morbidity and mortality from intubation for prolonged seizures [5]. The inaccurate diagnosis may also result in delayed psychological treatment for the issues underlying the attacks and social stigma associated with epilepsy. Previous research has found that over 75% of patients who are diagnosed as having PNES on VEM had been referred with a presumed diagnosis of epilepsy by their Neurologist [6]. It has been reported that on average, patients experiencing PNES are not correctly diagnosed until 7.2 years after the manifestation of the seizures. Such a long delay prior to the diagnosis of PNES clearly demonstrates the unsatisfactory nature of current procedures for evaluating this important group of patients [6].

The diagnosis between PNES and ES is the electrical discharge that can be monitored through a video electroencephalogram monitoring (VEM). In-patient VEM is the gold standard for distinguishing different types of seizures [7]. Although it has a high yield in diagnosis and management, it is expensive, time consuming and, labor and resource intensive [8]. It also requires inpatient admission, which adds a further burden on the healthcare system. Due to the widespread use of VEM machines for seizure categorization, it is safe to assume that visual cues (of motor seizures) captured by an expert observer give critical information on diagnosis and treatment planning in addition to EEG signals. The videos accompanying EEG clearly show the manifestation of distinguishable feature in motor activity. Any neurological problem affecting the motor neurons will result in the manifestation of the problem in one of the body parts, specifically in the limbs that can be captured by an accelerometer sensor. Due to economic feasibility and the tediousness of VEM, alternate methods are being researched to differentiate PNES and ES. In our previous work, we have shown that manifestation of epileptic and nonepileptic seizures is quite different in its motor activity [9]. Therefore, a motor activity monitoring device should be able to distinguish between ES and PNES.

Unobtrusive and ambulatory monitoring get more important in case of patients who suffer from nocturnal ES. These patients are highly susceptible to injury or even sudden death as

Manuscript received November 20, 2014; revised April 03, 2015; accepted June 09, 2015. Date of publication June 17, 2015; date of current version July 06, 2016.

J. Gubbi, S. Kusmakar, A. S. Rao, and M. Palaniswami are with the Department of Electrical and Electronic Engineering, The University of Melbourne, Parkville, Vic. 3010, Australia (e-mail: jgl@unimelb.edu; skusmakar@student.unimelb.edu.au; aravinda@student.unimelb.edu.au; palani@unimelb.edu.au).

B. Yan and T. O'Brien are with the Melbourne Brain Centre, Royal Melbourne Hospital, Department of Medicine, The University of Melbourne, Parkville, Vic. 3052, Australia (e-mail: bernard.yan@mh.org.au; obrientj@unimelb.edu.au).

Color versions of one or more of the figures in this paper are available online at http://ieeexplore.ieee.org.

Digital Object Identifier 10.1109/JBHI.2015.2446539

the seizure goes unnoticed to the caregivers, hence making automated detection of seizures a pivotal and, in many cases, a life-saving task. Clinical decision making is a hot area in biomedical engineering, and for automated detection of seizures, the first and the foremost step is the identification of the seizure event and activities which can mimic seizure or activities of daily living (referred to as normal activity in this work). The use of accelerometer for the detection of ES has been reported in [10]. It was found that it was possible to detect the stereotypical patterns for myoclonic, clonic, and tonic ES termed as simple motor seizures and distinguish them from normal movement using 3-D accelerometer attached to four limbs and chest [10]. This work was extended further in [11], where four different time-frequency and time-scale methods were investigated. Cuppens *et al.* [12] have focused on the identification of normal activity and activity that corresponds to seizure. Results from the work of Becq *et al.* [13] is promising, where they have shown that a high sensitivity and specificity of 80% and 95%, respectively, can be achieved in the detection of generalized tonic–clonic seizures from accelerometer data based on a simple entropy feature obtained from the norm of acceleration. However, it can be inferred from the results that there is a slight overlap between the seizure activities and other motor manifestations. This can be due to reasons attributed to patient physiology, placement of the sensor for data collection, and the type of the activity patient is doing. Another study shows that the accelerometer can detect the nocturnal frontal lobe seizures with a high level of sensitivity and specificity [14], and wearable accelerometer-based kinematic sensors are successfully used as a body sensor network for detection of the motor patterns of ES [15].

Recently, Ungureanu *et al.* [16] have proposed the use of a different sensor modality for detection of nocturnal ES, due to ambiguity on the placement of the accelerometer on the patient and to identify seizures that do not normally manifest as motor seizures. However, for unobtrusive and ambulatory monitoring of patients, the challenge is to have a device and a method with a minimum number of sensors. This reduces the power consumption and the patient endurance that multiple sensors cause. In our work, we have focused only on motor seizures. Patients with motor ES are under a higher risk of injury or harm during an ES or PNES event. Therefore, requiring early and correct diagnosis for directed treatment is essential.

The use of surface electromyography (sEMG) is also reported in the literature as a viable method for the development of automated algorithm for detection of seizures. Patel *et al.* [17] have shown the use of sEMG data collected in conjugation with accelerometer data using a wearable sensor. They showed that sEMG data aid in identification and discrimination of activity of daily living from seizure events. Correct identification of normal or activity of daily living is a critical step for the development of an automated algorithm for seizure detection as many activities of daily living contribute to false alarms. Further, Conradsen *et al.* [18] have shown the efficacy of sEMG in the automated detection of general tonic–clonic seizures with a very high sensitivity of 100% and a specificity of 1 false detection per day.

Seizures can be broadly classified into two types: convulsive and nonconvulsive. Convulsive seizures cause involuntary contraction of muscles and can be visually observed. Most of the work reported in the literature as discussed in the above paragraphs is targeted at detection and classification of simple motor seizures. In our previous work [9], we proposed an approach based on short-time Fourier transform of the accelerometer data. The data were recorded using a wrist-worn wired accelerometer device. It was observed that PNES displays a stable dominant frequency during the course of a seizure event. However, ES shows more variation in the evolution of dominant frequencies. Motivated by the initial results, an ambulatory convulsive seizure monitoring system has been reported in this paper. A fully automated system for detection and diagnosis of PNES has not yet been addressed in the literature. In this regard, the system employs a wrist-worn accelerometer system that records motor activity. A new algorithm for detection and classification of convulsive seizures is proposed. The novel system is implemented using a commercially available hand-held device and tested on patients undergoing VEM. The main contributions of this study are summarized as follows.

1) Accurate detection of PNES based on the occurrence of seizure is critical for avoiding unnecessary delay in treatment. Correct diagnosis of PNES is reported to be delayed by 7.2 years on average. An automated system has been developed for identification of PNES in convulsive patients using limb motion analysis.
2) Continuous and unobtrusive monitoring is a challenging task due to the amount of data that are collected. A new method for accurately identifying seizures from accelerometer signal is proposed. The algorithm has the ability to detect seizure-like activity that is present hidden inside vast amounts of normal data.
3) A new classification algorithm has been proposed for classifying ES and PNES using time-frequency analysis. The algorithm is tested with good results on patient data collected in a hospital setting.

II. Method

The proposed system consists of two stages, seizure detection and seizure classification, as shown in Fig. 1. The wrist-worn device is mounted on the patient continuously for several days when the patient is under observation in the VEM system. The movement data are collected uninterrupted over this period other than during the device change over period that lasts a few minutes. Due to the large volume of data collected, an algorithm for detecting seizures accurately is developed in the first stage using time-domain features and k-means clustering. In the second stage, seizure activities are classified into ES or PNES with the help of discrete wavelet transform (DWT) and SVMs. In this section, the details are presented.

A. Data Collection and Processing

An ambulatory wireless system has been proposed that allows continuous monitoring and in the subject's natural setting. A smart-device application was developed for collecting the

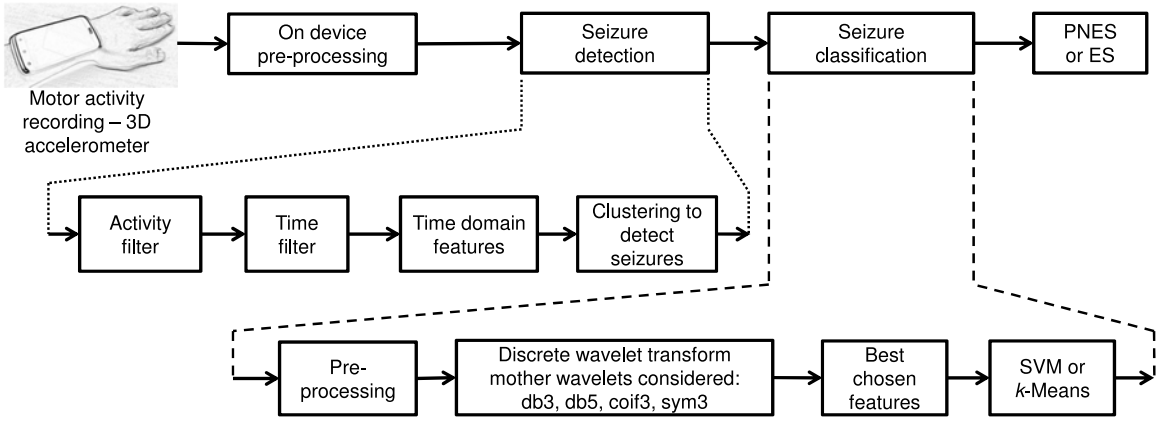

Fig. 1. Flowchart of the proposed method. The method consists of four stages of processing. In the first stage, data are collected from a wrist-worn accelerometer. In the second stage, a filter that eliminates small movements has been implemented as on-device processing. Seizure detection is the third stage comprising of four steps: activity filter, time filter, extraction of time-domain features, and clustering of detected features. In the final stage, the seizure is classified as PNES or ES. For classification of events as PNES of ES, an initial preprocessing of the signals is performed on the signals from seizure detection stage, followed by extraction of wavelet features (db3, db5, coif3, and sym4) and then classification using k-means and SVMs.

TABLE I
OVERALL NUMBER OF PATIENTS WHO HAD SEIZURES DURING THE MONITORING DURATION WITH THE NUMBER OF ES, PNES, AND BOTH ES AND PNES PATIENTS

	Overall	ES	PNES	Both ES and PNES
Patients	27	10	3	1
Observed events	85	21	13	–
Age	34.44 ± 13.34	32.80 ± 13.40	39.33 ± 18.61	30.00 ± 0.00
Male	$8(29.6\%)$	$5(50.00\%)$	0.00	0.00
Female	$19(70.30\%)$	$5(50.00\%)$	3 (100%)	1 (100%)
Duration of events (sec)	117 ± 123	115 ± 111.6	224 ± 203.43	–

A total of 14 patients had convulsive events. Only patients with convulsive events are shown with patient age and event duration represented as mean $\pm$ standard deviation. Number of males and female patients and their respective percentages shown in brackets for each category.

movement data. Apple iPod Touch with an accelerometer sensor was used for all our experiments. Two iPods (one for each hand) were attached firmly to the patient's wrists with elastic armbands to prevent unintended movements. Each device consisted of an MEMS accelerometer $(\pm 2.5\ \mathrm{g})$. A simple filter to detect activity was used in order to conserve energy. The device was changed every 12 h due to battery drainage. The raw accelerometer data were stored using flash memory on the device and later transferred to the computer for analysis. The sampling frequency of the data collected was 50 Hz and each packet contained values along three axes and a time stamp. The data were collected during 2012 and 2013 among patients in the epilepsy video telemetry unit at the Royal Melbourne Hospital in Melbourne, Australia, who experienced motor seizures during hospitalization. Human Research Ethics Committee approval was obtained from the Royal Melbourne Hospital (HREC Project 300.259). The study was conducted in keeping with the regulations established by the hospital. During the stay in the hospital, the patients underwent VEM continuously for at least three days, and at the same time, the patients had an accelerometer device fitted firmly to both their wrists. The devices were time synchronized with VEM setup in order to ensure exact comparison and analysis, by manually autoupdating the time on both the devices from same network. A lag of few milliseconds in registrations of VEM and accelerometer device is permissible according to clinical experts. Moreover, the EEG technicians manually annotate the accelerometer data for the different seizure types. The EEG technicians performed the annotation without any automated signal processing. The annotation was performed by visual assessment of the accelerometer data using MATLAB. The EEG technicians reported that similar clues of seizure-like activity is present on accelerometer data as seen on EEG during VEM. Patients were excluded from this study for three reasons: 1) if the seizures were absent (i.e., no movement); 2) if they suffered from significant underlying psychoses (preventing informed consent); and 3) the monitoring was intracranial. Summary of the data collected is shown in Table I. Out of a total 57 subjects recruited, 27 patients had seizures during VEM recording. Using the VEM, 85 events were observed that included 34 convulsive events (14 patients) and 51 nonconvulsive events (13 patients). This study focuses on convulsive patients only as motor activity monitoring is possible only if it manifests on a body part; hence, convulsive events are considered. Out of 14 convulsive patients, ten epileptic patients and three nonepileptic patients were encountered. One patient had both epileptic and nonepileptic seizure events. A total of 21 ES

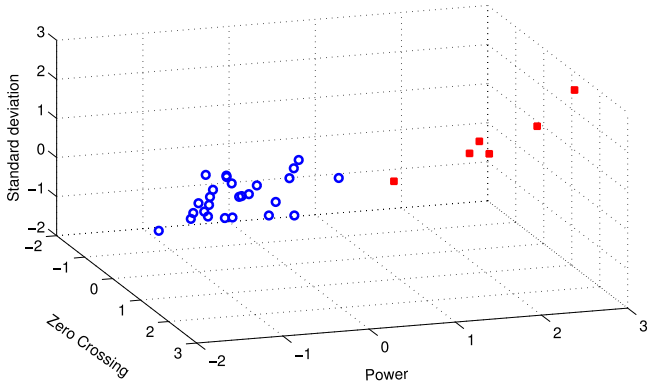

Fig. 2. Example of k-means clustering using standard deviation, zero crossing, and power of the resultant acceleration signal. ○ indicates normal activities and □ indicates seizure events for patient no. 1. From the figure, it is clear that standard deviation, zero crossing, and power are sufficient to cluster the events as normal or seizure-like events.

events and 13 PNES events were identified using VEM. Based on the feedback from the specialists, a minimum event length of 20 s is considered in this study as an event. This resulted in a reduction of the number of events captured by the device, and there are 14 ES events and five PNES events for detection and classification. Although the number of events is lesser, it should be noted that the analysis is performed on events of different window lengths (5 s in classification stage) resulting in a sizeable number of samples. In effect, eight convulsive patients are available for analysis with a total of nineteen events. The mean duration of ES and PNES events were 115 and 224 s, respectively. More details about the data can be seen in Table I.

B. Detection of Seizure Events

Accurate detection of seizure events is the first step in analysis of the motor movement that comprises of vast amounts of data. A simple time- and frequency-domain approach is proposed for detection of seizure activity. There are three possibilities of output at this stage: 1) no activity; 2) normal arm movements; and 3) seizure activity. The resultant signal used at the first stage is calculated using $R = \sqrt{x^2 + y^2 + z^2}$. The resultant is then preprocessed using a simple activity filter that declares all signals less than 0.2 g as no activity or normal activity. The value of 0.2 g is empirically chosen and is based on the lower bound of the collected seizure data. Although this value is heuristical, logically it is fair to accept it due to the nature of the physiology of seizures. Followed by the use of the threshold, the signal of 20-s length with 50% overlap is filtered using a sixth-order Butterworth bandpass filter with 2 and 25 Hz as cutoff frequencies. This will filter all spurious spikes and some of the controlled arm movements, which is not the nature of ES. Cuppens *et al.* [14] have shown the use of such preprocessing steps, where they have used low-pass filter with cutoff frequency of 47 Hz, whereas in our work, we have focused on a particular frequency range based on our observations of dominant frequency of typical seizure events from our previous work [9]. Seizure activities of minimum length of 20 s are considered in this work, and hence, the choice of 20 s windows is made. A fast Fourier

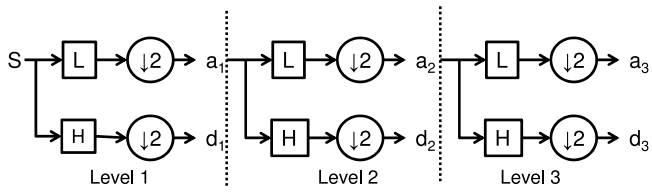

Fig. 3. Three-level Wavelet decomposition. S is the input signal. H is the high-pass filter and L is the low-pass filter. $\downarrow 2$ indicates downsampling by a factor of 2. a_i is the approximate coefficient and d_i is the detailed coefficient. In the proposed work, six-level wavelet decomposition is performed, resulting in an approximate coefficient along with six detailed coefficients.

transform (FFT) of the filtered signal is calculated by dividing the 20-s window into 20 blocks of 1 s each. The magnitude of the dominant peak along with the corresponding frequencies is calculated. A detailed analysis of the mean and standard deviation of the magnitude and frequency is performed. It is found that the normalized peak magnitude of the data during the seizure has a lower bound of 0.009, and the upper bound on the peak magnitude during normal activity is several order lesser than 0.009. Hence, it is chosen as the threshold in our activity filter. Further, it is observed that for at least 10 s, out of the 20-s window, the activity is high in magnitude during the seizure, which is not the case in majority of the normal activity. This will ensure that all subtle movements are excluded from seizure-like activities, hence the name activity filter. A similar observation has been made by Cuppens *et al.* [12] in their very recent work, where they have reported that activities that manifest for lesser than 10 s are most likely normal nocturnal movements. After preprocessing, the filtered data now contain normal activity that has significant acceleration in addition to seizures. As mentioned earlier, only events that have a minimum duration of 20 s are considered in our work. Followed by the activity filter, we use the time filtering to remove normal and seizure events that have duration of less than 20 s. At the end of time filtering, we are left with arm movements that comprise of normal events and seizure events with the number of normal activities significantly higher than seizure activities. The thresholds are justified as we are not eliminating any seizure-like activity but only focus on removing very obvious normal movements. In order to extract only seizure events from this biased set, k-means clustering is employed on time-domain features that are extracted. The 15 time-domain features extracted include signal power, zero crossings, energy, measures of central tendency (mean, median, mode), measures of dispersion (interquartile range, standard deviation, amplitude), skewness, kurtosis, and entropy (Shannon, log energy, norm, threshold). Features were calculated for signals corresponding to x-, y-, and z-axes of accelerometer and also for the resultant signal R. In total, we had a feature set comprising of 60 features. Out of the 60 time-domain features, signal power, zero crossing, and standard deviation were selected as key features based on feature evaluation using variance as the criterion in agreement with Cuppens *et al.* [14]. For each subject, the duration of events is represented by time window $T = \{t_1, t_2, \ldots, t_n | t_I = 1 \text{ s}\}$. The feature vector for a particular subject comprising of t_n windows is generated using the 60 features. Let $U = [u_1, u_2, \ldots, u_{60}]$

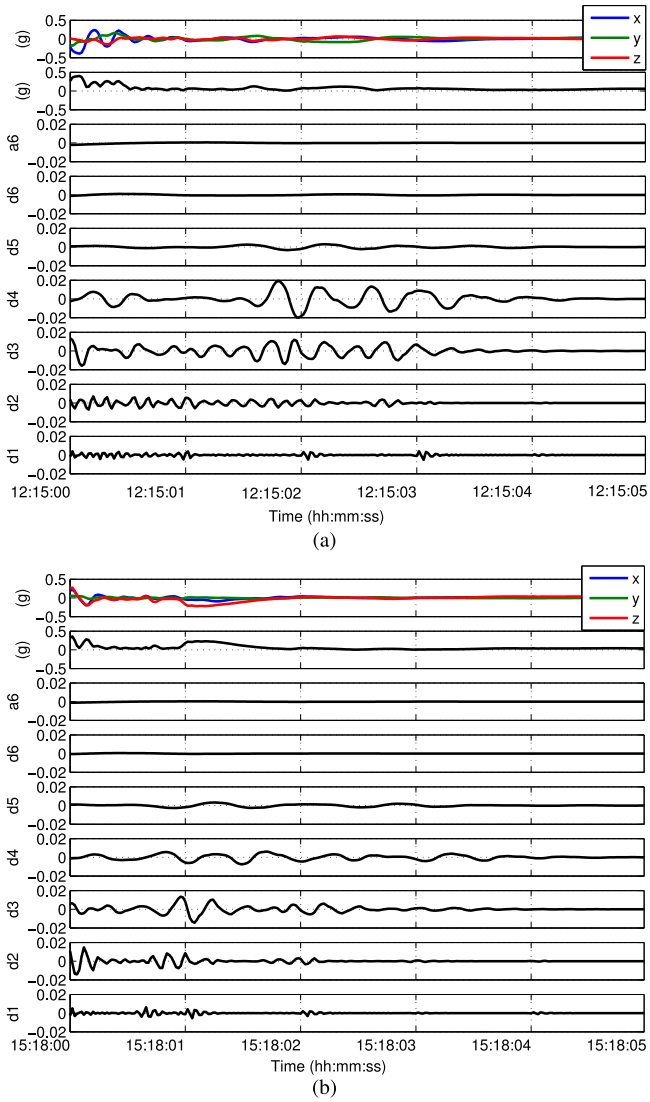

Fig. 4. Six levels of wavelet decomposition shown for (a) PNES and (b) ES during respective events. In each of the graphs, the first subgraph shows the input acceleration signals corresponding to x-, y-, and z-axes and the subsequent subgraph show the resultant axis derived from x-, y-, and z-axes. The subsequent graphs show the six levels of detailed coefficients and an approximate coefficient. The results were obtained using the db5 coefficient.

represent the feature vector for a particular subject and the corresponding event. This is reduced to $V = [v_1, v_2, v_3]$, where v_1, v_2, and v_3 correspond to the power, zero crossing, and standard deviation of the resultant.

k-means [19] is an unsupervised clustering algorithm that classifies the multivariate data into k clusters, where the number of clusters k is known *a priori*. The intuition is to identify k centroids based on the input data. The k centroids then form the centroid of each cluster. Ideally, the centroids must be far apart from each other, and the data points are associated with one of the nearest k centroids. The k-means clustering is an iterative algorithm, and thus, the procedure of newly formed clusters with k centroids is iterated until convergence (cluster centroids become fixed and data points associated also become fixed). This can be written as minimizing an objective function

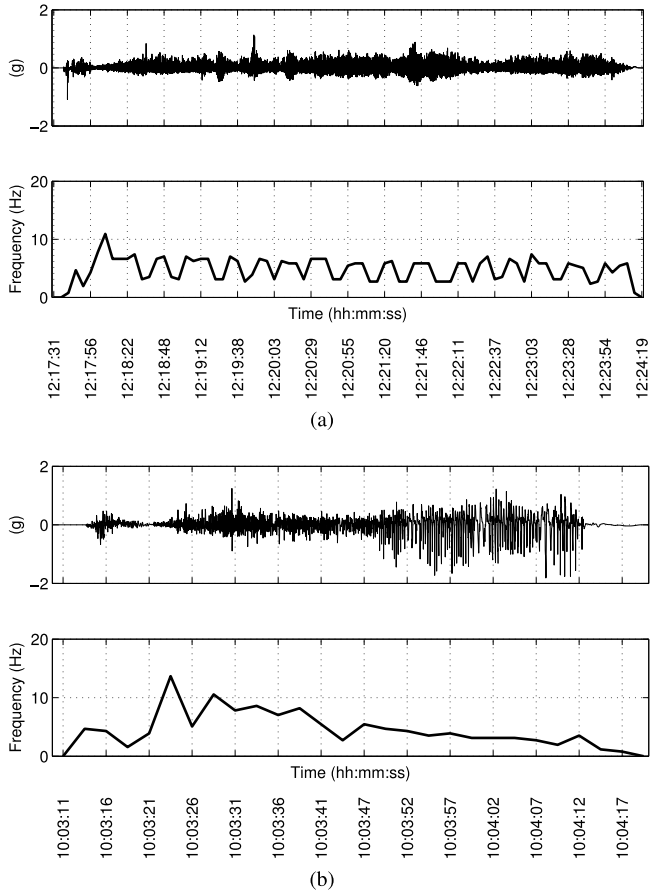

Fig. 5. Resultant accelerometer signal and evolution of dominant frequency during (a) PNES and (b) ES from [9].

as

$$Q = \arg\min_{k} \sum_{j=1}^{k} \sum_{i=1}^{n} \|x_i - c_j\|^2 \tag{1}$$

where x_i are the n data points and c_j are the k cluster centroids.

In the present scenario, the data contain n observations for a single subject. Each observation consists of three features. These features must be divided into two clusters: normal events and seizure events. The k-means clustering will divide the input vectors into a larger group of normal events and another smaller group of seizure events as shown in Fig. 2. In Fig. 2, $\circ$ represents the normal activity and $\square$ represents the seizure events. As can be inferred from Fig. 2, the data are clearly divided into two distinct clusters and all the seizure events correspond to outliers in our data.

C. Classification of Seizure Into Epileptic and Pseudo Nonepileptic Events

Our initial work as a proof of principle [9] demonstrated the feasibility of differentiating ES and PNES using a single-stage frequency analysis. Using a wired accelerometer and continuous collection of the data, the collected acceleration signals were analyzed using a Fourier transform and the first dominant peak was analyzed. It was found that the variation of the first

TABLE II
EVENT DETECTION RESULTS FOR EIGHT CONVULSIVE PATIENTS, FOR A TOTAL OF 19 EVENTS CAPTURED USING THE WRIST-WORN ACCELEROMETER DEVICE

Patient Number	Event Number	Observed start time (hh:mm:ss)	Predicted start time (hh:mm:ss)	Start time error (sec)	Observed duration (sec)	Predicted duration (sec)	Duration Error (sec)
1	1	16:04:00	16:04:31	+31	66	60	−6 (9.1%)
	2	00:33:00	00:33:07	+07	66	48	−18 (27.2%)
	3	07:23:49	07:23:47	−02	58	49	−9 (15.5%)
	4	10:03:00	10:03:37	+37	68	59	−9 (13.2%)
	5	14:42:00	14:42:41	+41	52	51	−1 (1.9%)
	6	16:12:00	16:12:33	+33	51	47	−4 (7.8%)
2	1	04:50:35	04:50:46	+11	105	44	−61 (58.1%)
3	1	15:23:53	15:22:35	−78	83	32	−51 (61.4%)
	2	03:07:12	03:06:46	−26	60	42	−18 (30.0%)
4	1	15:08:38	15:08:09	−29	156	34	−125 (78.2%)
	2	15:32:33	15:32:27	−05	115	58	−57 (49.5%)
	3	11:52:15	11:51:24	−51	68	32	−36 (52.9%)
5	1	21:15:00	21:16:49	+109	434	307	−125 (29.2%)
	2	11:20:00	11:21:19	+79	495	498	+3 (0.8%)
	3	12:20:00	12:18:00	−120	660	269	−391 (59.2%)
	4	12:35:00	12:32:50	+130	363	369	−6 (1.6%)
6	1	00:45:00	00:48:28	+208	500	64	−449 (89.8%)
7	1	12:06:09	12:06:26	+17	70	59	−11 (15.7%)
8	1	23:40:00	23:45:04	+304	85	58	−27 (31.7%)

The table highlights the observed start time (with respect to VEM), accelerometer capture start time, and error. Similarly, the event duration observed (with respect to VEM), accelerometer data, and error are shown.

TABLE III
PERFORMANCE OF THE PROPOSED EVENT DETECTION ALGORITHM

Patient No.	Sensitivity	Specificity	Accuracy
1	100	96.15	96.88
2	100	58.82	59.22
3	100	93.94	94.12
4	100	91.30	92.30
5	100	100.00	100.00
6	100	73.33	75.00
7	100	72.62	72.94
8	100	100.00	100.00

The table shows the results of seizure event detection approach for eight patients that comprised of 19 convulsive events.

dominant frequency between patients with ES and PNES varied considerably with high coefficient of variation in dominant frequency of ES events as compared to PNES events. In contrast to our earlier work, we use wireless accelerometer that can be worn without any hindrance to normal activity. Further, due to the nature of data preprocessing, the data collected are accurate but sparse. As a result, the algorithm based on FFT [9] proposed earlier is not robust. In order to gain convenience in data collection, some sacrifice is necessary in the quality of the data collected, but we attempt to compensate it by proposing a new algorithm based on time-frequency analysis and SVM classifier. The classifier is build using fivefold cross-validation, where four folds are used for training the classifier and fifth fold is used to test the model. This approach results in a completely automated system that can detect seizure events and diagnose PNES accurately that is a step further to what has been reported earlier [9].

1) Extraction of Wavelet Features: Analysis of nonstationary functions can be performed using mathematical functions that allow simultaneous localization of interesting patterns in time and scale. Wavelets belong to this class of functions and they decompose the data into different frequency bands. Each component is analyzed with a resolution matched to its scale. They also offer important properties such as linearity and orthogonality that can be used for implementing the algorithm on wearable devices that are resource hungry and work in real time. The DWT further enhances their use in DSP chips by operating on input data vectors whose length is an integer power of two. A DWT is calculated by filtering followed by down sampling by a factor of 2 as shown in Fig. 3. It is clear from Fig. 3 that wavelets provide multiscale representation of the input signal. In Fig. 3, the approximate coefficient a_j and detailed coefficient d_j are calculated using (2) and (3), where h and l are high-pass and low-pass filter coefficients, respectively:

$$a_{j+1}[p] = \sum_{n=-\infty}^{n=\infty} l[n-2p]a_j[n] \tag{2}$$

$$d_{j+1}[p] = \sum_{n=-\infty}^{n=\infty} h[n-2p]a_j[n]. \tag{3}$$

Several mother wavelets with different orders were analyzed. Finally, a small subset of mother wavelets including daubechies (db3, db5), coiflets (coif3), and symlet (sym4) were empirically chosen for detailed analysis and validation of the proposed method. Fig. 4 shows the decomposed signal with six detailed coefficients and one approximate coefficient. Using power as the criterion, detailed coefficients at level 2 (d_2), 3 (d_3), and 4 (d_4) were chosen for further analysis. In addition, the approximate coefficients (a_6) after six-level wavelet decomposition was used. The entropy and power of each 5-s window (with 50% overlap) in a seizure were calculated for d_2, d_3, d_4, and a_6. The coefficient of variation of power and entropy for each event was

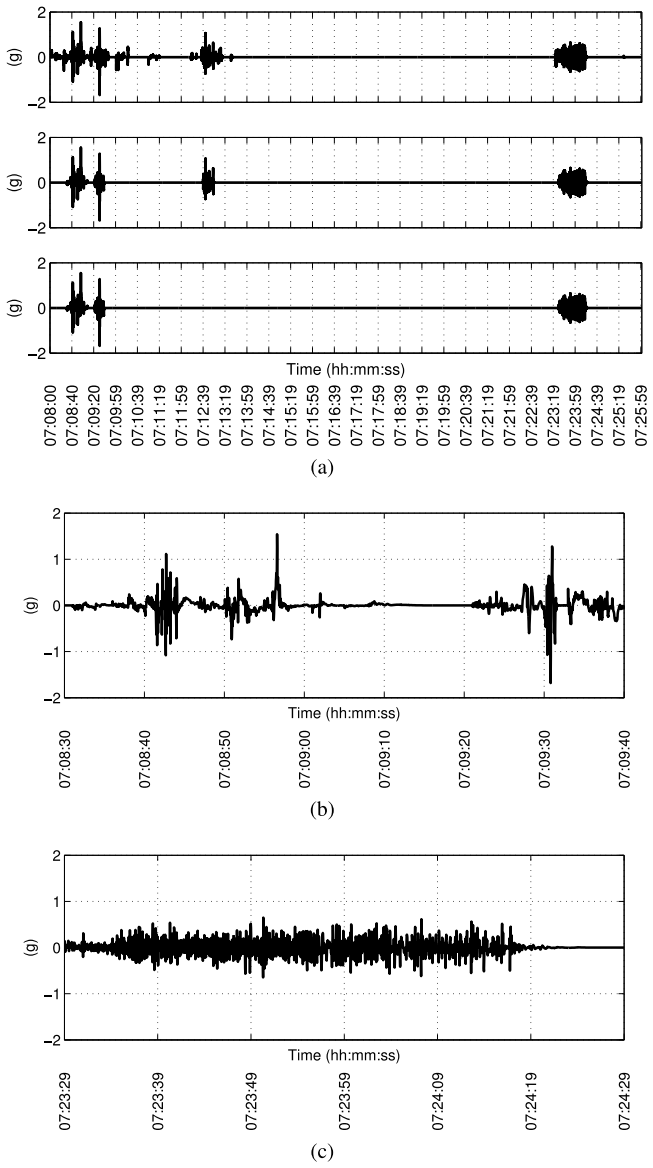

Fig. 6. Results of event detection stage for patient no. 1. (a) Data with normal activity and ES event (top most), result of activity filtering (second subplot), and result of time filtering (third subplot). (b) Normal activity (enlarged view of the left most activity from (a), third subplot). (c) Seizure-like event (enlarged view of the right most activity from (a), third subplot).

calculated and used as a feature for classification. This resulted in a feature vector of length of eight made up of coefficients of variation in power (d_2, d_3, d_4, a_6) and entropy (d_2, d_3, d_4, a_6).

2) Classification Using Unsupervised Learning: Based on our earlier work [9], we hypothesize that the coefficient of variation of power and entropy in different frequency bands should provide the basis for classifying PNES from ES. As reported by Bayly *et al.* [9], PNES exhibit stable dominant frequency during the course of the event (leading to low coefficient of variation) as against evolving dominant frequency in ES (leading to the high coefficient of variation). In order to achieve this, k-means has been used with a cluster center initialization algorithm (CCIA) [20]. Due to the nature of k-means by using the random centroid initialization, the algorithm fails to work consistently and also the data characteristics are not efficiently utilized. Density-based multiscale condensation strategy has been used in this work [20] by using a derived attribute of mean and standard deviation of the data. CCIA generates $\acute{k}$ clusters where $\acute{k} > k$. The idea of the algorithm is to merge nearby clusters from the pool of $\acute{k}$ clusters based on Euclidian distance between cluster centers. The new cluster centers formed by this procedure will be used as initial cluster centers for the k-means algorithm. The same procedure is repeated for d_2, d_3, d_4, and a_6.

3) Classification Using SVMs: SVMs [21] are a class of trained models used in data analysis and pattern recognition for classification and regression. The models are learned using the supervised learning where the input data and output class are labeled. Internally, the SVMs use the *Kernel Methods* [22], [23], where the algorithm depends only on the inner-product of the data. Consequently, the properties of the *kernel function* determines the dot product of the data. This inner-product feature space is a high-dimensional space and SVMs can effectively generate nonlinear decision boundaries to generate accurate classification results. The kernel functions are also advantageous to handle data that do not have fixed vector structure. In this work, radial basis function (RBF) kernel is used. The RBF kernel for two input data samples is given by

$$K(x, x') = \exp\Big(- \frac{\|x - x'\|_2^2}{2\sigma^2} \Big) \tag{4}$$

where x and x' are input data points and σ is the bandwidth of the RBF kernel. In this work, based on empirical evidence during the training stage, the RBF kernel parameters (C, γ) were set to $C = 1$ and $\gamma = 0.25$, where C is the penalty parameter and $\gamma = \frac{1}{2\sigma^2}$. The parameter C is a penalty term used in optimization of decision boundary and controls the classification error [24].

III. Results and Discussion

The mode of data collection and the device used in this work is different as explained earlier. Hence, as a first evaluation, we verify our results with Bayly *et al.* [9] who have used first dominant frequency within 2.56-s windows for the length of the event. In the context of this work, it should be noted that the data collection is using a sensor with lower sensitivity and there is a filter within the device that suppresses very low strength signal. This will allow us to ensure that the basic characteristic of the signal that is needed to classify ES and PNES is not lost. The results of dominant frequency evolution during the events are shown in Fig. 5. As can be seen, consistent with the earlier result, we observe little change in the case of PNES and vast change in the case of ES. Based on this, we employed more sophisticated signal-processing techniques to extract features with higher discriminating capability. As shown in Table IVc, leave-one-out error (LOOE) of 6.67% and an overall accuracy of 92% are achieved in PNES classification using the approach presented in this work, which shows a vast improvement over the previous results [9].

The results of the event detection stage are summarized in Table II. All events are detected out of the 19 analyzed events.

TABLE IVA
RESULTS OF EVENT (PNES) CLASSIFICATION

Data	Mother Wavelet	Accuracy	Sensitivity	Specificity	f-score	LOOE
Resultant	db3	84.00 ± 26.08	80.00 ± 32.60	100.00 ± 0.00	0.85 ± 0.26	13.33
X		68.00 ± 22.80	65.00 ± 28.50	80.00 ± 44.72	0.73 ± 0.22	23.33
Y		76.00 ± 21.91	70.00 ± 27.39	100 ± 0.00	0.79 ± 0.23	16.66
Z		84.00 ± 16.73	80.00 ± 20.92	100.00 ± 0.00	0.88 ± 0.14	13.33
Resultant	db5	92.00 ± 10.95	90.00 ± 13.69	100.00 ± 0.00	0.94 ± 0.08	6.66
X		68.00 ± 17.89	65.00 ± 22.36	80.00 ± 44.72	0.74 ± 0.20	30
Y		84.00 ± 8.94	80.00 ± 11.18	100.00 ± 0.00	0.89 ± 0.06	13.33
Z		88.00 ± 10.95	85.00 ± 13.69	100.00 ± 0.00	0.91 ± 0.08	10
Resultant	coif3	76.00 ± 16.73	75.00 ± 17.68	80.00 ± 44.72	0.83 ± 0.13	20
X		68.00 ± 10.95	70.00 ± 11.18	60.00 ± 54.77	0.78 ± 0.08	26.66
Y		92.00 ± 10.95	90.00 ± 13.69	100.00 ± 0.00	0.94 ± 0.08	6.66
Z		84.00 ± 8.94	80.00 ± 11.18	100.00 ± 0.00	0.89 ± 0.06	16.66
Resultant	sym3	84.00 ± 16.73	85.00 ± 13.69	80.00 ± 44.72	0.89 ± 0.11	13.33
X		80.00 ± 14.14	85.00 ± 13.69	60.00 ± 54.77	0.87 ± 0.09	20
Y		88.00 ± 10.95	85.00 ± 13.69	100.00 ± 0.00	0.91 ± 0.08	13.33
Z		84.00 ± 8.94	80.00 ± 11.18	100.00 ± 0.00	0.89 ± 0.06	16.66

k-means classifier performance using sub-band power as the feature for different mother wavelets. LOOE (Leave one out error).

TABLE IVB
RESULTS OF EVENT (PNES) CLASSIFICATION

Data	Mother Wavelet	Accuracy	Sensitivity	Specificity	f-score	LOOE
Resultant	db3	76.00 ± 8.94	75.00 ± 0.00	80.00 ± 44.72	0.84 ± 0.05	20
X		68.00 ± 17.89	65.00 ± 22.36	80.00 ± 44.72	0.74 ± 0.20	30
Y		88.00 ± 10.95	85.00 ± 13.69	100.00 ± 0.00	0.91 ± 0.08	13.33
Z		84.00 ± 16.73	85.00 ± 22.36	80.00 ± 44.72	0.88 ± 0.14	23.33
Resultant	db5	80.00 ± 0.00	75.00 ± 0.00	100.00 ± 0.00	0.86 ± 0.00	16.66
X		72.00 ± 10.95	70.00 ± 11.18	80.00 ± 44.72	0.80 ± 0.09	23.33
Y		76.00 ± 16.73	70.00 ± 20.92	100.00 ± 0.00	0.81 ± 0.14	20
Z		84.00 ± 8.94	85.00 ± 13.69	80.00 ± 44.72	0.89 ± 0.06	13.33
Resultant	coif3	76.00 ± 8.94	70.00 ± 11.18	100.00 ± 0.00	0.82 ± 0.09	20
X		88.00 ± 10.95	90.00 ± 13.69	80.00 ± 44.72	0.92 ± 0.07	13.33
Y		80.00 ± 20.00	80.00 ± 20.92	80.00 ± 44.72	0.85 ± 0.15	23.33
Z		68.00 ± 10.95	60.00 ± 13.69	100.00 ± 0.00	0.74 ± 0.10	30
Resultant	sym3	72.00 ± 10.95	65.00 ± 13.69	100.00 ± 0.00	0.78 ± 0.10	20
X		56.00 ± 21.91	50.00 ± 17.68	80.00 ± 44.72	0.64 ± 0.19	70
Y		92.00 ± 10.95	90.00 ± 13.69	100.00 ± 0.00	0.94 ± 0.08	13.33
Z		76.00 ± 8.94	80.00 ± 11.18	60.00 ± 54.77	0.84 ± 0.05	23.33

k-means classifier performance using subband entropy as the feature for different mother wavelets.

The predicted start time is also fairly accurate other than for patient no. 6. In terms of the duration of prediction, a mixed set of result is reported. The goal at this stage was to detect the event, and the duration of the event is not a major hurdle. By designing a simple extension filter, it is possible to get more accurate event duration if required. Table III gives the accuracy, sensitivity, and specificity obtained by the proposed event detection scheme. As intended, the sensitivity of the proposed algorithm is excellent with 100% results. Although some false alarms are detected in a few patients, a closer analysis revealed very low intensity single seizure as the primary reason for these patients. However, the threshold chosen ensures that the events are not missed, which is the original goal.

Fig. 6 shows stepwise result of event detection stage for patient no. 1. The top most plot in Fig. 6 show a section of the data with normal activity and seizure-like activity. At this stage, the algorithm should output only seizure like activity. As explained in methodology, an activity filtering is performed and the results are shown in Fig. 6(a), middle. As can be seen, low intensity activities that involve normal movement are filtered. Time filtering is performed and the output is shown in Fig. 6(a), bottom. It is clear that only the event (on extreme right) and some high intensity normal activity (extreme left) are remaining at this stage that needs to be classified. Finally, k-means clustering is used to detect events of interest that classifies normal activity [see Fig. 6(b)] and seizure events [see Fig. 6(c)].

Tables IVa–IVd summarize the results of event classification stages using different feature–classifier combinations for various mother wavelets and accelerometer axis. f-score and LOOE are also reported. As can be seen from Table IVc, SVM using db5 mother wavelet and subband power as the feature results in the best f-score and lowest LOOE consistently than other

TABLE IVc
RESULTS OF EVENT (PNES) CLASSIFICATION

Data	Mother Wavelet	Accuracy	Sensitivity	Specificity	f-score	LOOE
Resultant	db3	84.00 ± 26.08	80.00 ± 32.60	100.00 ± 0.00	0.85 ± 0.26	13.33
X		80.00 ± 24.49	75.00 ± 30.62	100.00 ± 0.00	0.82 ± 0.25	16.66
Y		88.00 ± 26.83	85.00 ± 33.54	100 ± 0.00	0.88 ± 0.27	10
Z		88.00 ± 17.89	85.00 ± 22.36	100 ± 0.00	0.90 ± 0.15	10
Resultant	db5	92.00 ± 10.95	90.00 ± 13.69	100.00 ± 0.00	0.94 ± 0.08	6.66
X		92.00 ± 10.95	90.00 ± 13.69	100.00 ± 0.00	0.94 ± 0.08	6.66
Y		92.00 ± 10.95	90.00 ± 13.69	100.00 ± 0.00	0.94 ± 0.08	6.66
Z		88.00 ± 17.89	90.00 ± 13.69	80.00 ± 44.72	0.92 ± 0.11	10
Resultant	coif3	84.00 ± 16.73	85.00 ± 13.69	80.00 ± 44.72	0.89 ± 0.11	13.33
X		72.00 ± 17.89	75.00 ± 17.68	60.00 ± 54.77	0.80 ± 0.13	23.33
Y		92.00 ± 10.95	90.00 ± 13.69	100 ± 0.00	0.94 ± 0.08	6.66
Z		92.00 ± 10.95	90.00 ± 13.69	100.00 ± 0.00	0.94 ± 0.08	10
Resultant	sym3	84.00 ± 16.73	85.00 ± 13.69	80.00 ± 44.72	0.89 ± 0.11	13.33
X		80.00 ± 14.14	85.00 ± 13.69	60.00 ± 54.77	0.87 ± 0.09	23.33
Y		92.00 ± 10.95	90.00 ± 13.69	100.00 ± 0.00	0.94 ± 0.08	10
Z		88.00 ± 10.95	85.00 ± 13.69	100 ± 0.00	0.91 ± 0.08	13.33

SVM classifier performance using subband power as the feature for different mother wavelets.

TABLE IVd
RESULTS OF EVENT (PNES) CLASSIFICATION

Data	Mother Wavelet	Accuracy	Sensitivity	Specificity	f-score	LOOE
Resultant	db3	88.00 ± 17.89	90.00 ± 13.69	80.00 ± 44.72	0.92 ± 0.11	6.66
X		84.00 ± 16.73	85.00 ± 13.69	80.00 ± 44.72	0.89 ± 0.11	13.33
Y		88.00 ± 10.95	85.00 ±	100 ± 0.00	0.91 ± 0.08	16.66
Z		92.00 ± 10.95	90.00 ± 13.69	100.00 ± 0.00	0.94 ± 0.08	10
Resultant	db5	88.00 ± 10.95	90.00 ± 13.69	80.00 ± 44.72	0.92 ± 0.07	13.33
X		96.00 ± 8.94	95.00 ± 11.18	100.00 ± 0.00	0.97 ± 0.06	10
Y		88.00 ± 17.89	85.00 ± 22.36	100.00 ± 0.00	0.90 ± 0.15	13.33
Z		88.00 ± 10.95	90.00 ± 13.69	80.00 ± 44.72	0.92 ± 0.07	10
Resultant	coif3	84.00 ± 8.94	90.00 ± 13.69	60.00 ± 54.77	0.90 ± 0.06	16.66
X		84.00 ± 8.94	90.00 ± 13.69	60.00 ± 54.77	0.90 ± 0.06	16.66
Y		80.00 ± 20.00	80.00 ± 20.92	80.00 ± 44.72	0.85 ± 0.15	20
Z		80.00 ± 14.14	80.00 ± 20.92	80.00 ± 44.72	0.85 ± 0.12	26.66
Resultant	sym3	88.00 ± 10.95	85.00 ± 13.69	100.00 ± 0.00	0.91 ± 0.08	13.33
X		76.00 ± 16.73	70.00 ± 20.92	100.00 ± 0.00	0.81 ± 0.14	26.66
Y		84.00 ± 16.73	80.00 ± 20.92	100.00 ± 0.00	0.88 ± 0.14	16.66
Z		92.00 ± 10.95	90.00 ± 13.69	100.00 ± 0.00	0.94 ± 0.08	10

SVM classifier performance using subband entropy as the feature for different mother wavelets.

feature–classifier pair and mother wavelets. In the event classification stage, the training model was validated by a fivefold cross-validation. The results as shown in Tables IVc and IVd suggest that fifth-order Daubechies wavelet gives the best results, which also correlates well with the findings of Nijsen *et al.* [11]. Similar results can be inferred from Tables IVa and IVb, where classification has been done using k-means. Further, it is seen that a high f-score is found for signal corresponding to z-axis and the resultant signal, which suggests that most of the seizure-like activities manifest in the direction of z-axis, and the resultant signal shows better results as it is a combined effect of the signals in all three axes. However, it should be noted that there happens to be no clear direction of movement corresponding to the z-axis when the accelerometer recording is a fully free form. As a result, there is no easy way to attribute the movement to any specific arm muscle.

Fig. 7 shows the observed and predicted value for patient no. 4 and exhibits both epileptic and nonepileptic seizures. The data were collected during August 27, 2012 to August 30, 2012. Fig. 7(a) shows the observed data and Fig. 7(b) shows the predicted data. The gap in raw data on August 29, 2012 indicate that the device was not worn or the battery was drained out until the following morning. Normal activity in Fig. 7(a) is absent as the information was not available in VEM, but the prediction shows normal activity that was significant as declared by the event detection stage of the proposed algorithm.

This study demonstrates the use of a wrist-worn accelerometer for detecting convulsive seizure events and classifying them as ES or PNES. Bayly *et al.* [9] used FFT transform and showed that the PNES events featured a stable dominant frequency and ES characterized an evolving dominant frequency and was proven that an accelerometer device can be used as a diagnostic

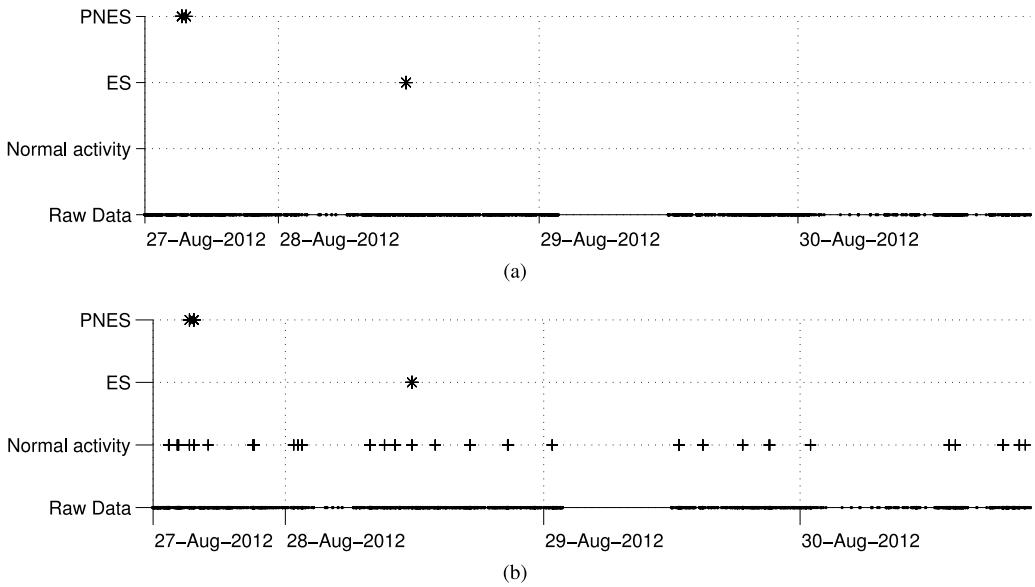

Fig. 7. (a) Observed and (b) predicted events for patient no. 4 collected over three days. The patient had both ES and PNES.

tool. In this work, wavelet features have been used; furthermore, k-means and SVM have been used for detection and classification of PNES events. The localization of time and frequency using wavelet provides a higher resolution frequency and scale analysis of the accelerometer signals. In line with this, the window size of the wavelet decomposition is reduced from 2.56 to 1 s.

From Table III, it is clear that the algorithm has a sensitivity of 100% for all the patients, which clearly demonstrates the strength of the proposed approach. For any seizure detection algorithm, it is vitally important that no seizure goes undetected but at the same time to minimize the number of false alarms. Our efforts have been to incorporate these concepts into the development of an automated algorithm and come up with an accurate seizure detection and classification system. Our algorithm performed fairly well with a near perfect event detection sensitivity of 100% and a specificity of 85.77% for the 19 convulsive events. The stage 1 of the proposed methodology has shown promising and motivating results for seizure event detection, clearly stating the reliability of the wrist-worn accelerometer devices in detecting seizure events. One of the patients (patient no. 2) had a lot of false positives which contributed to the overall reduction of specificity; otherwise, the algorithm was able to detect seizure events with good accuracy as seen from Table III. For patient no. 2, the VEM recording of the patient was monitored as there were a high number of false positives. The possible reason can be attributed to the improper placement of the device or loose strap of the device. In these cases, even slight movement of the hands will result in activity data with higher amplitude and frequency.

Table II shows the observed time of the seizure (for all events), which is the time of seizure on VEM and the predicted time of the seizure, which is the time of the seizure on the wrist-worn accelerometer device. The positive start time error denotes the latency in motor manifestation of the seizure event. In accordance from the VEM recordings of the patient, it is seen that the latency is the result of the gradual increase in motor manifestations which starts off as a subtle event and manifests gradually. These subtle movements at the start of the events mostly get filtered out during the on-device processing of the data in event detection stage, thus resulting in latency. For patient no. 8, a huge delay was observed. The reasons were attributed to error introduced due to the time synchronization between iPod touch and the PC. Further reasons were attributed to the posture of the patient during VEM recording, resulting in loosening of the device strap affecting the duration and timing of the recorded event on device; however, the occurrence of such mishaps was observed to be rare. Table II also shows the duration error, which is found to be negative in all cases except for event no. 2 in patient no. 5, where the predicted duration is greater by 3 s. This can be due to the subsiding nature of the convulsive manifestations of the seizure event as it terminates; however, the electrical activity of the brain has completely subsided. The reason for shorter predicted duration in most of the cases is ascribed to the fact that when a typical convulsive seizure starts and subsides, it is mostly followed by the subtle limb movements (the typical observation made from the VEM data). Such subtle limb movements are filtered on the device during event detection stage and thus rendering equivalent to no motor manifestations by the proposed algorithm. Thus, the observed duration is higher in most of the cases in comparison to the predicted seizure duration.

The future direction involves in investigating whether the acceleration data from a single axis are sufficient for seizure detection. However, the seizure detection is a multifactorial problem in that the seizures involve complex motor manifestations and the orientation of the accelerometer device is continuously changing. In this direction, the motion analysis of the trajectory of the patient's arm during a typical seizure using a wrist-based accelerometer coupled with another sensor and finding proxy accelerometer coordinate system to aid accurate diagnosis is

required. Beniczky *et al.* [25] have performed the analysis of sEMG in ES and PNES. Motor seizure causes involuntary contraction of muscles and performing a study determining the accelerometer axes responsible for those muscle activation will further help in minimizing the false positives and increasing the accuracy of the proposed method. This is achieved by considering the activity only in a particular accelerometer axis and discarding the data with minimal activity in the corresponding axis.

However, an ambulatory monitoring device for seizure detection based on accelerometery can have the following limitations.

1) The accuracy of seizure detection can vary with the placement of the device on the arm, as the algorithm is developed for a wrist-worn device.
2) Since we have considered seizures of durations greater than 20 s, any seizures of lesser duration will go undetected.
3) Furthermore, the system is still to be validated in home conditions. For now, the system is tested and developed in hospital settings, where patients do not engage in lot of activities, which will not be the case in real-home situations.

IV. Conclusion

A wireless wearable device for detecting and diagnosing pseudo nonepileptic seizure is proposed. A novel algorithm for detection of seizures using time-domain features is developed. The detected seizures are classified into epileptic and nonepileptic seizures using wavelet features and SVM classifier. The data from patients undergoing video EEG monitoring are collected using the wearable device and tested on convulsive patients with excellent results. The results demonstrate the feasibility of using an automated easy-to-wear device to detect and diagnose PNES in primary clinical setting.

Acknowledgment

The authors would like to thank D. Fernando and C. Muller for their feedback and help during data collection as part of their honors thesis. The authors would also like to thank the staff of Royal Melbourne Hospital and the patients who agreed to be a part of this study.

Disclosure: None of the authors has any conflict of interest to disclose.

References

[1] World Health Organization. (2014, Feb.). What are neurological disorders? [Online]. Available: http://www.who.int/features/qa/55/en/

[2] S. Noachtar and A. Peters, "Semiology of epileptic seizures: A critical review," *Epilepsy Behaviour*, vol. 15, no. 1, pp. 2–9, 2009.

[3] S. R. Benbadis, K. Johnson, K. Anthony, G. Caines, G. Hess, C. Jackson, F. L. Vale, and W. O. Tatum, "Induction of psychogenic nonepileptic seizures without placebo," *Neurology*, vol. 55, no. 12, pp. 1904–1905, 2000.

[4] N. Bodde, J. Brooks, G. Baker, P. Boon, J. Hendriksen, and A. Aldenkamp, "Psychogenic non-epileptic seizures diagnostic issues: A critical review," *Clin. Neurol. Neurosurgery*, vol. 111, no. 1, pp. 1–9, 2009.

[5] M. Reuber and C. E. Elger, "Psychogenic nonepileptic seizures: Review and update," *Epilepsy Behavior*, vol. 4, no. 3, pp. 205–216, 2003.

[6] R. C. Martin, F. G. Gilliam, M. Kilgore, E. Faught, and R. Kuzniecky, "Improved health care resource utilization following video-EEG-confirmed diagnosis of nonepileptic psychogenic seizures," *Seizure*, vol. 7, no. 5, pp. 385–390, 1998.

[7] M. Reuber, G. Fernandez, J. Bauer, C. Helmstaedter, and C. Elger, "Diagnostic delay in psychogenic nonepileptic seizures," *Neurology*, vol. 58, no. 3, pp. 493–495, 2002.

[8] J. Alving and S. Beniczky, "Diagnostic usefulness and duration of the inpatient long-term video-EEG monitoring: Findings in patients extensively investigated before the monitoring," *Seizure*, vol. 18, no. 7, pp. 470–473, 2009.

[9] J. Bayly, J. Carino, S. Petrovski, M. Smit, D. A. Fernando, A. Vinton, B. Yan, J. R. Gubbi, M. S. Palaniswami, and T. J. O'Brien, "Time-frequency mapping of the rhythmic limb movements distinguishes convulsive epileptic from psychogenic nonepileptic seizures," *Epilepsia*, vol. 54, no. 8, pp. 1402–1408, 2013.

[10] T. M. Nijsen, J. B. Arends, P. A. Griep, and P. J. Cluitmans, "The potential value of three-dimensional accelerometry for detection of motor seizures in severe epilepsy," *Epilepsy Behavior*, vol. 7, no. 1, pp. 74–84, 2005.

[11] T. M. Nijsen, R. M. Aarts, P. J. Cluitmans, and P. A. Griep, "Time-frequency analysis of accelerometry data for detection of myoclonic seizures," *IEEE Trans. Inf. Technol. Biomed.*, vol. 14, no. 5, pp. 1197–1203, Sep. 2010.

[12] K. Cuppens, P. Karsmakers, A. Van de Vel, B. Bonroy, M. Milosevic, S. Luca, T. Croonenborghs, B. Ceulemans, L. Lagae, S. Huffel, and B. Vanrumste, "Accelerometry-based home monitoring for detection of nocturnal hypermotor seizures based on novelty detection," *IEEE J. Biomed. Health Informat.*, vol. 18, no. 3, pp. 1026–1033, May 2014.

[13] G. Becq, P. Kahane, L. Minotti, S. Bonnet, and R. Guillemaud, "Classification of epileptic motor manifestations and detection of tonic–clonic seizures with acceleration norm entropy," *IEEE Trans. Biomed. Eng.*, vol. 60, no. 8, pp. 2080–2088, Aug. 2013.

[14] K. Cuppens, L. Lagae, B. Ceulemans, S. Van Huffel, and B. Vanrumste, "Detection of nocturnal frontal lobe seizures in pediatric patients by means of accelerometers: A first study," in *Proc. Annu. Int. Conf. IEEE Eng. Med. Biol. Soc.*, 2009, pp. 6608–6611.

[15] A. Dalton, S. Patel, A. R. Chowdhury, M. Welsh, T. Pang, S. Schachter, G. OLaighin, and P. Bonato, "Development of a body sensor network to detect motor patterns of epileptic seizures," *IEEE Trans. Biomed. Eng.*, vol. 59, no. 11, pp. 3204–3211, Nov. 2012.

[16] C. Ungureanu, V. Bui, W. Roosmalen, R. Aarts, J. Arends, R. Verhoeven, and J. Lukkien, "A wearable monitoring system for nocturnal epileptic seizures," in *Proc. 8th Int. Symp. Med. Inform. Commun. Technol.*, Apr. 2014, pp. 1–5.

[17] S. Patel, C. Mancinelli, A. Dalton, B. Patritti, T. Pang, S. Schachter, and P. Bonato, "Detecting epileptic seizures using wearable sensors," in *Proc. IEEE 35th Annu. Northeast Bioeng. Conf.*, 2009, pp. 1–2.

[18] I. Conradsen, S. Beniczky, K. Hoppe, P. Wolf, and H. B. Sorensen, "Automated algorithm for generalized tonic–clonic epileptic seizure onset detection based on sEMG zero-crossing rate," *IEEE Trans. Biomed. Eng.*, vol. 59, no. 2, pp. 579–585, Feb. 2012.

[19] J. MacQueen, "Some methods for classification and analysis of multivariate observations," in *Proc. 5th Berkeley Symp. Math. Statistics Probab.*, California, CA, USA, 1967, vol. 1, pp. 281–297.

[20] S. S. Khan and A. Ahmad, "Cluster center initialization algorithm for k-means clustering," *Pattern Recog. Lett.*, vol. 25, no. 11, pp. 1293–1302, 2004.

[21] B. E. Boser, I. M. Guyon, and V. N. Vapnik, "A training algorithm for optimal margin classifiers," in *Proc. 5th Annu. Workshop Comput. Learning Theory*, 1992, pp. 144–152.

[22] B. Scholkopf and A. J. Smola, *Learning with Kernels: Support Vector Machines, Regularization, Optimization, and Beyond*. Cambridge, MA, USA: MIT Press, 2001.

[23] J. Shawe-Taylor and N. Cristianini, *Kernel Methods for Pattern Analysis*. Cambridge, U.K.: Cambridge Univ. Press, 2004.

[24] K.-P. Wu and S.-D. Wang, "Choosing the kernel parameters for support vector machines by the inter-cluster distance in the feature space," *Pattern Recog.*, vol. 42, no. 5, pp. 710–717, 2009.

[25] S. Beniczky, I. Conradsen, M. Moldovan, P. Jennum, M. Fabricius, K. Benedek, N. Andersen, H. Hjalgrim, and P. Wolf, "Quantitative analysis of surface electromyography during epileptic and nonepileptic convulsive seizures," *Epilepsia*, vol. 55, pp. 1128–1134, 2014.

Jayavardhana Gubbi (SM'15) received the Bachelor of Engineering degree from Bangalore University, Bengaluru, India, in 2000, the Ph.D. degree from the University of Melbourne, Parkville, Australia, in 2007.

For three years, he was a Research Assistant at the Indian Institute of Science, where he was involved in speech technology for Indian languages. He is currently a Research Fellow in the Department of Electrical and Electronic Engineering, The University of Melbourne. From 2010 to 2014, he was an ARC Australian Postdoctoral Fellow Industry working on an industry linkage grant in video processing. His current research interests include video processing, Internet of Things, and ubiquitous healthcare devices. He has coauthored more than 40 papers in peer-reviewed journals, conferences, and book chapters over the last ten years. He has served as conference secretary and publications chair in several international conferences in the area of wireless sensor networks, signal processing, and pattern recognition.

Shitanshu Kusmakar (S'14) received the B.Tech. degree from Thapar University, Punjab, India, in 2010, and the M.Tech. degree in clinical engineering from the Indian Institute of Technology Madras, Chennai, India, in 2012. He has been working toward the Ph.D. degree in the Department of Electrical and Electronic Engineering, The University of Melbourne, Parkville, Australia, since December 2013.

For a year, he was a Clinical Applications Engineer at R&D Centre HTIC, set up by the Indian Institute of Technology Madras and Department of Biotechnology (DBT), Government of India. His research interests include ubiquitous health monitoring devices, biomedical signal processing, epilepsy, classification, and pattern recognition.

Aravinda S. Rao (S'09) received the B.E. degree in electronics and communications engineering from Visveswaraya Technological University, Belgaum, India, in 2006, and the M.E. degree in electronics and telecommunications from Deakin University, Geelong, Australia, in 2010. He is currently working toward the Ph.D. degree at the University of Melbourne, Parkville, Australia, working on video-based monitoring crowd and understanding behavior.

He was a Deputy Engineer in the Development and Engineering division of Naval Systems/Sonar Systems, focusing on designing and developing hardware for submarine sonar systems, at Bharat Electronics Limited, Bangalore, India, during 2006–2007. He commenced his research studies at the Department of Electrical and Electronic Engineering, The University of Melbourne, in 2011. His research interests include computer vision, crowd behavior analysis, manifold learning, wireless sensor networks, and embedded systems design.

Bernard Yan received F.R.A.C.P. degree from College of Physicians, in 2003 and M.B.B.S. degree from the University of Melbourne, Parkville, Australia, in 1994.

He is an Assistant Professor in the Department of Medicine, The University of Melbourne, and the Department of Neurology, Royal Melbourne Hospital since 2005. He has published 106 academic papers in peer-reviewed medical journals. He is actively involved in investigator-driven and industry-sponsored multicenter clinical trials. He is the Principal Investigator of several international studies in cerebrovascular diseases. He pursued his academic interest in cerebrovascular disease research. One of his key research interests is in the development of portable mobile wireless sensors for the monitoring of patients with neurological diseases.

Terence O'Brien (M.B.B.S. Melb., M.D. Melb., F.R.A.C.P.) is The James Stewart Chair of Medicine, The Department of Medicine, The Royal Melbourne Hospitals, and consultant neurologist at The Royal Melbourne Hospital, Victoria, Australia. He leads a large translational research team undertaking both basic studies, involving animal models, and clinical studies. He is a specialist in neurology and clinical pharmacology, with particular expertise in epilepsy, anti-epileptic drugs and in-vivo imaging in animal models and humans. He did his clinical and research training at St. Vincent's and Royal Melbourne Hospitals in Melbourne, and then the Mayo Clinic, Rochester, Minnesota, USA (1995–1998). His research is broad based, covering both basic and clinical studies related to epilepsy, traumatic brain injury and other neurodegenerative conditions. The work has had two primary goals: First to better understand the determinants of treatment response, identify biomarkers for treatment outcomes–imaging, electrophysiological, genomic and clinical, and develop new treatment approaches. Second to investigate the fundamental neurobiological basis, and inter-relationship, of the neuropsychiatric co-morbidities present in many patients with epilepsy and neurodegenerative conditions. He has published over 275 peer-reviewed original papers in leading scientific and medical journals, and 20 other publication.

Marimuthu Palaniswami (F'12) received the B.E. (Hons.) from the University of Madras, Chennai, India, the M.E. degree from the Indian Institute of Science, Bengaluru, India, and the Ph.D. degree from the University of Newcastle, Callaghan, Australia.

He then joined the University of Melbourne, Parkville, Australia, where he is currently a Professor of electrical engineering and Director/Convener of a large ARC Research Network on Intelligent Sensors, Sensor Networks and Information Processing with about 200 researchers and interdisciplinary themes as focus for the center. He has coauthored more than 340 refereed journal and conference papers, including a number of books, edited volumes, and book chapters. His research interests include smart sensors and sensor networks, machine learning, neural networks, support vector machines, signal processing, biomedical engineering, and control.

Dr. Palaniswami has served international boards and advisory committees including a panel member for National Science Foundation, as an Associate Editor for Journals/transactions including IEEE TRANSACTIONS ON NEURAL NETWORKS and *Computational Intelligence for Finance*. He is the Subject Editor for the *International Journal on Distributed Sensor Networks*. He was given a Foreign Specialist Award by the Ministry of Education, Japan, in recognition of his contributions to the field of machine learning.